Crystal and magnetic structures of the superconductor $CeNi_{0.8}Bi_2$

K. Kodama,[1,2] S. Wakimoto,[1,2] N. Igawa,[1] S. Shamoto,[1,2] H. Mizoguchi,[3] and H. Hosono[3,4]

[1]*Quantum Beam Directorate, Japan Atomic Energy Agency, Tokai, Ibaraki 319-1195, Japan*
[2]*JST, Transformative Research-Project on Iron Pnictides (TRIP), Tokyo 102-0075, Japan*
[3]*Frontier Research Center, Tokyo Institute of Technology, Nagatsuta, Yokohama 226-8503, Japan*
[4]*Materials and Structures Laboratory, Tokyo Institute of Technology, Nagatsuta, Yokohama 226-8503, Japan*

We have performed powder neutron diffraction on the new superconductor, $CeNi_{0.8}Bi_2$ with a superconducting transition temperature $T_c \sim 4.2$ K. The structural parameters of this compound at room temperature are determined by Rietveld analysis. Below about 5 K, the clear magnetic Bragg peaks with propagation vector $q = (0\ 0\ 0)$ are observed. The observed intensities of magnetic Bragg peaks can be explained by the magnetic structure that the two Ce moments in the unit cell are antiparallel along the c axis. The magnetic Bragg peaks are observed in the superconducting state, indicating the coexistence of the antiferromagnetic ordering and the superconductivity in this compound. The intensity of magnetic Bragg peak monotonously increases with decreasing temperature below T_N and does not exhibit apparent anomaly at T_c, obviously different from cases of heavy fermion superconductors in which the magnetic ordering and the superconductivity coexist, for example, Cd-doped $CeCoIn_5$. These results suggest that the $4f$ electron of the Ce atom is not coupled with the superconducting carrier, and the magnetic ordering is almost independent of the superconductivity in $CeNi_{0.8}Bi_2$.

I. INTRODUCTION

An iron-based superconductor was first discovered in the LaFeAsO system with a so-called ZrCuSiAs-type structure whose superconductivity is induced by partial substitution of fluorine for oxygen.[1] After this discovery, the development of new materials with an Fe layer in which the superconductivity is considered to appear, has been performed, resulting in the discoveries of other iron-based superconductors, such as the so-called 122 system,[2] $FeSe_{1-x}Te_x$,[3] LiFeAs,[4] and so on. On the other hand, new superconductors with a ZrCuSiAs-type structure which consist of elements other than Fe are also explored, for example, $La_{1-x}Sr_xNiAsO$.[5] Recently, Mizoguchi and his collaborators have discovered the superconductivity in $CeNi_{0.8}Bi_2$ with a superconducting transition temperature of $T_c \sim 4.2$ K.[6]

Series compounds $CeMBi_2$ and $CeMSb_2$ have ZrCuSiAs-type structures with space group of $P4/nmm$ corresponding to the so-called 1111 system, where M is a transition metal element such as Mn, Fe, Ni, Cu, Ag, and so on.[7] For $CeMBi_2$, Bi_1, M, Ce, and Bi_2 sites correspond to As, Fe, rare-earth element, and O sites, respectively. The "parent" compound of $CeNi_{0.8}Bi_2$, $CeNiBi_2$, is a moderately heavy fermion antiferromagnet; magnetic ordering appears at about 5 K and the electronic specific heat coefficient γ is relatively large (470 mJ/K^2 mol).[8] This parent compound does not exhibit a superconductivity although the electric conductivity is metallic down to the lowest temperature.[8,9]

The superconductivity is induced by the deficiency of the Ni atom,[6] as the superconductivity in the iron-based superconductor of the so-called 1111 system is induced by oxygen deficiency.[10] The resistivity and superconducting shielding signal in the magnetic field show the superconducting transition at about 4.2 K. At about 5 K, specific heat C exhibits a jump of $\sim$4 J/K mol. This jump may be attributed to the magnetic ordering of the Ce $4f$ moment because the entropy estimated by an integration of C/T below

5 K corresponds to $R \ln 2$, which is expected from the twofold degenerated ground state of the Ce $4f$ electron. The clear jump of the specific heat is not observed at around T_c because the jump caused by the superconducting transition is much smaller than the jump caused by the magnetic ordering, suggesting that the charge carrier which causes the superconductivity is not coupled with the Ce $4f$ electron and the mass is not enhanced.[6]

If the Ce $4f$ electron is coupled with the superconducting carrier in the present compound, the magnetic fluctuation of $4f$ electron can induce the unconventional superconducting order parameter. In such a case, the temeprature dependence of the magnetic Bragg peak should have some anomaly at T_c. Then we have performed powder neutron diffraction measurements on $CeNi_{0.8}Bi_2$ in order to investigate the existence of the coupling between the Ce $4f$ electron and the superconducting carrier. First, we present the structural parameters determined by Rietveld analysis in Sec. III A. The electronic state of this compound discussed in Ref. 6 is based on the present result. In Sec. III B, we report the magnetic structure and the temperature dependence of the ordered moment of the Ce $4f$ moment. Our results suggest that the Ce $4f$ electron does not contribute to the superconductivity in this compound, consistent with the suggestion in Ref. 6.

II. EXPERIMENTS

For the compound of $CeNi_xBi_2$, we found through a series of synthesis experiments that samples synthesized by conventional solid state reaction have a constant Ni deficiency of $x = 0.8$.[6] A powder sample of $CeNi_{0.8}Bi_2$ for the present neutron measurements was prepared by following method. Ce, Ni, and Bi, powders with a nominal composition of $CeNi_{0.8}Bi_2$ were used as starting materials. The mixed powder was evacuated in a silica tube and heated at 500 °C for 10 h and 750 °C for 20 h. The obtained powder was ground and pressed into pellets, and it was heated at 800 °C for 10 h in

the evacuated silica tube. Inductively coupled plasma (ICP) spectroscopy was used to confirm the chemical composition, $CeNi_{0.8}Bi_2$, which was consistent with the nominal composition. The sample appears stable thermally in a dry box or an evacuated glass tube, but decomposes in an hour when exposed to an ambient atmosphere. This decomposition would be induced by the reaction of an unusual valence state of Bi ions in the material with water vapor in the atmosphere. Thus, we paid attention so as to avoid decomposition or degradation of the sample. The sample of about 14.3 g was used in neutron diffraction measurements. Electric resistivity and superconducting shielding measurements confirm that the T_c value and a volume fraction of shielding signal are the same as the values reported in Ref. 6.

The powder neutron diffraction pattern for the analysis on a crystal structure was collected by using the high-resolution powder diffractometer (HRPD) installed in reactor JRR-3 of the Japan Atomic Energy Agency (JAEA). The neutron wavelength was 1.8234 Å and the collimation was open (effective value of 35')-40'-S-6' (S denotes sample). The pattern was collected at room temperature. The powder sample was set in a vanadium holder enclosed in Al cans filled with He gas in order to avoid the decomposition in the atmosphere. Diffraction data for the analysis on the magnetic structure were collected by using triple-axes spectrometer TAS-2 in reactor JRR-3 of JAEA. The neutron wavelength used was 2.3590 Å and the collimation was 14'-40'-S-40'-80'. The sample enclosed in the Al can was mounted in a closed-cycle refrigerator.

III. RESULTS AND DISCUSSIONS

A. Analysis of crystal structure

Figure 1 shows the neutron powder diffraction pattern of $CeNi_{0.8}Bi_2$ obtained from the HRPD. The observed data

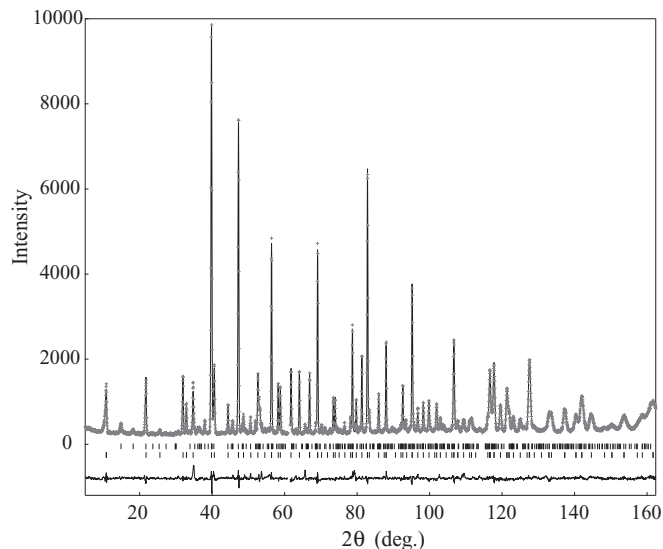FIG. 1. Observed (crosses) and calculated (solid lines) neutron powder diffraction pattern of $CeNi_{0.8}Bi_2$. The observed pattern is collected by using the HRPD at room temperature. Vertical bars show the calculated position of Bragg reflections including the impurities. The solid line at the bottom of the figure is the difference between observed and calculated intensities.

TABLE I. Atomic positions of $CeNi_{0.8}Bi_2$ (space group $P4/nmm$) determined by Rietveld analysis of neutron powder diffraction data at room temperature. Obtained lattice parameters are $a = 4.5439(1)$ and $c = 9.6414(2)$ Å. The R factor, R_{wp}, is 6.04 %

Atom	Site	Occ.	x	y	z	B (Å^2)
Ce	$2c$	1	1/4	1/4	0.2691(3)	0.83(4)
Ni	$2b$	0.8	3/4	1/4	1/2	1.83(4)
Bi$_1$	$2c$	1	1/4	1/4	0.6384(2)	0.92(3)
Bi$_2$	$2a$	1	3/4	1/4	0	0.66(4)

are shown by crosses. Structural analysis on the neutron powder diffraction pattern is performed by using the program RIETAN2000.[11] The space group of $P4/nmm$ is used because we know that the series compounds of $CeMBi_2$ and $CeMSb_2$ have the same structures, as shown in Sec. I. The diffraction pattern is analyzed including $NiBi_3$, $NiBi$, and Ni as impurities. Because a small peak which cannot be assigned by the above impurities is observed at $2\theta \sim 61.2°$, the intensity data in the 2θ range of $60.9°$–$61.5°$ are excluded in the analysis. The occupation factor of Ni is fixed at 0.8 which is determined by ICP spectroscopy. The obtained structural parameters of $CeNi_{0.8}Bi_2$ are shown in Table I. The errors of the parameters shown in the table are mathematical standard deviations obtained by the analysis. The diffraction pattern calculated by using refined parameters is shown in Fig. 1 by solid lines. The calculated line can reproduce the observed data. Mass fractions of the impurities are 9.1% for $NiBi_3$, 1.4% for $NiBi$, and 0.8% for Ni, respectively. The larger thermal parameter of Ni relative to other sites may be due to the impurities.

B. Magnetic structure and T dependence of an ordered Ce moment

Results of the 2θ scan at 11.2 and 2.9 K, obtained from TAS-2, are shown in Fig. 2(a) by gray and black lines, respectively. At 2.9 K a clear Bragg peak appears on the right-hand side of 002 reflection, corresponding to 100 reflection. The intensities of 102 and 111 reflections are slightly enhanced at 2.9 K. These results show the existence of magnetic ordering at lower temperatures and the coexistence of magnetic ordering and the superconductivity. Figure 2(b) shows the intensity obtained by subtracting the intensity at 11.2 K from the intensity at 2.9 K. Clear magnetic Bragg peaks are observed at lower temperatures at the reciprocal lattice points corresponding to 100, 102, 111, and 201. The data are scattered around $2\theta \sim 53°$ and $63°$, due to large nuclear Bragg intensities of 112/103 and 113/200 reflections whose intensities are about 70 000 and 50 000 counts at their peak positions, respectively. Magnetic 113 reflection does not have clear peak profile due to the large experimental error mentioned above, although it should have almost the same intensity as the magnetic 201 reflection in the magnetic structure presented below.

From these results, we can consider the magnetic structure at low temperatures. For $10l$ reflections, the clear magentic Bragg peaks are observed at $l = 2n$ and they are nearly absent at $l = 2n + 1$, indicating that the magnetic moments of two Ce atoms in a unit cell at (1/4 1/4 0.2691) and (3/4 3/4 0.7309)

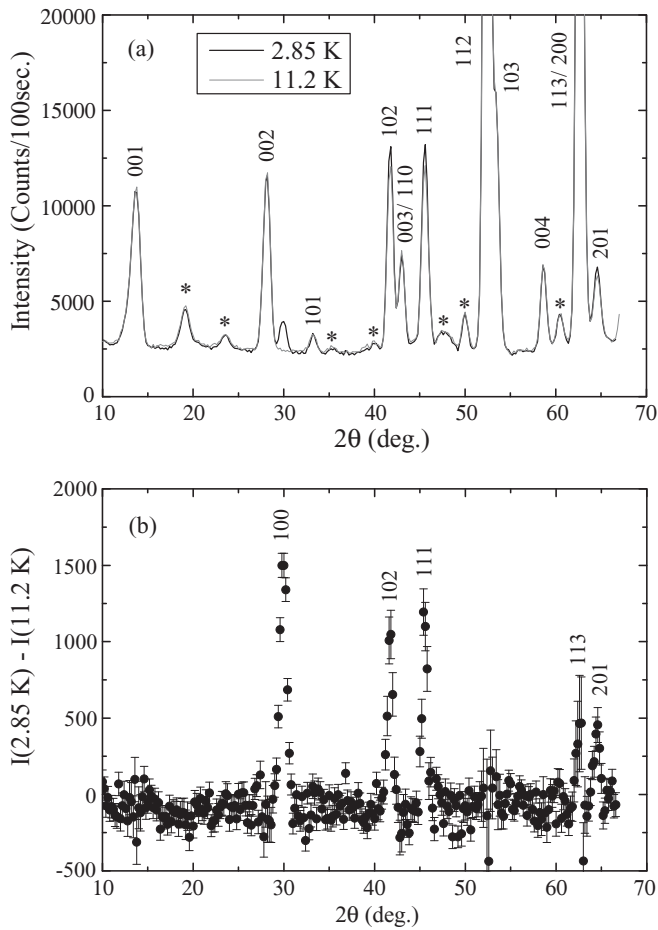FIG. 2. (a) Neutron powder diffraction patterns of $CeNi_{0.8}Bi_2$ obtained at 11.2 K (gray line) and 2.9 K (black line). The data are collected by using TAS-2. Miller indices are shown for nuclear Bragg peaks. The peaks marked by asterisks are contributed from impurities, for example, $NiBi_3$. (b) Magnetic Bragg intensity obtained by subtracting the intensity at 11.2 K from the intensity at 2.9 K.

are antiparallel. This intensity modulation of magnetic 10*l* reflections against *l* also shows that Ni moments are almost independent of the observed magnetic Bragg peaks even if the Ni atoms have magnetic moments. The scattering intensity from the Ni moments should not depend on *l* because two Ni atoms are located on a flat layer at $z = 1/2$. In magnetic susceptibility measurements, the contribution of the Ni atom to the Curie–Weiss-like susceptibility is nearly absent.[8,12] These results suggest that the Ni atom is nonmagnetic. The clear peaks are not observed at 00*l* positions in Fig. 2(b). If the Ce moments are perpendicular to the *c* axis, magnetic 00*l* reflections with $l = 2n + 1$ must have large intensities. Especially, the intensity of 001 reflection is expected to be about four times as large as the intensity of 100 reflection. The absence of magnetic 00*l* reflections indicates that the two Ce moments are oriented along the *c* axis. It is consistent with the anisotropy of the magnetic susceptibility, indicating that the antiferromagnetic easy axis is the *c* axis.[8] Then we can get the magnetic structure shown in Fig. 3. In the figure, the Ce atom at (1/4 1/4 0.2691) is located at the origin.

The integrated intensities of observed nuclear and magnetic Bragg reflections, I_{obs}, are shown in Table II. The former
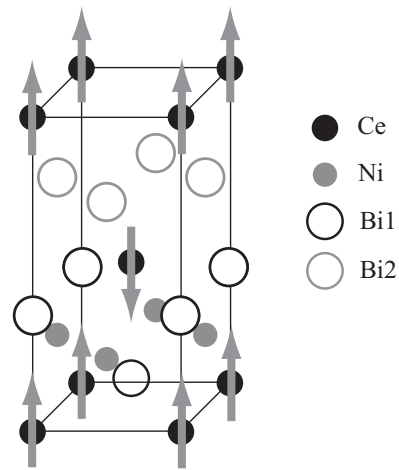

FIG. 3. Crystal and magnetic structures of $CeNi_{0.8}Bi_2$. The Ce atom at (1/4 1/4 0.2691) is the origin. Gray arrows show the magnetic moments of Ce atoms.

intensities are estimated by using the diffraction data at 11.2 K and the latter ones are estimated by using the data shown in Fig. 2(b). The intensities of nuclear Bragg reflections calculated by using the structural parameters shown in Table I, I_{cal}, are also shown in right hand side of I_{obs} in the table. The calculated intensities almost correspond with the observed intensities. To estimate the ordered moment of Ce sites at 2.9 K, the intensities of magnetic reflections obtained from the magnetic structure shown in Fig. 3 are fitted to the observed intensities by using a least-squares fitting program. The estimated value of the ordered moment is 1.43(5) μ_B. Here, we use the isotropic magnetic form factor of Ce^{3+}.[13] The calculated intensities of magnetic Bragg reflections are shown in the right-hand side of the table. The calculated intensities agree with the observed intensities, indicating that the present magnetic structure and the obtained ordered moment are reasonable. Although 113 reflection should have the intensity

TABLE II. Observed and calculated intensities of nuclear (left hand side) and magnetic (right-hand side) Bragg peaks. Calculated intensities are obtained by using the structural parameters shown in Table I. In the calculation of magnetic Bragg intensity, we use the amplitude of the Ce moment of 1.43 μ_B and the isotropic magnetic form factor of Ce^{3+} Ref. 13.

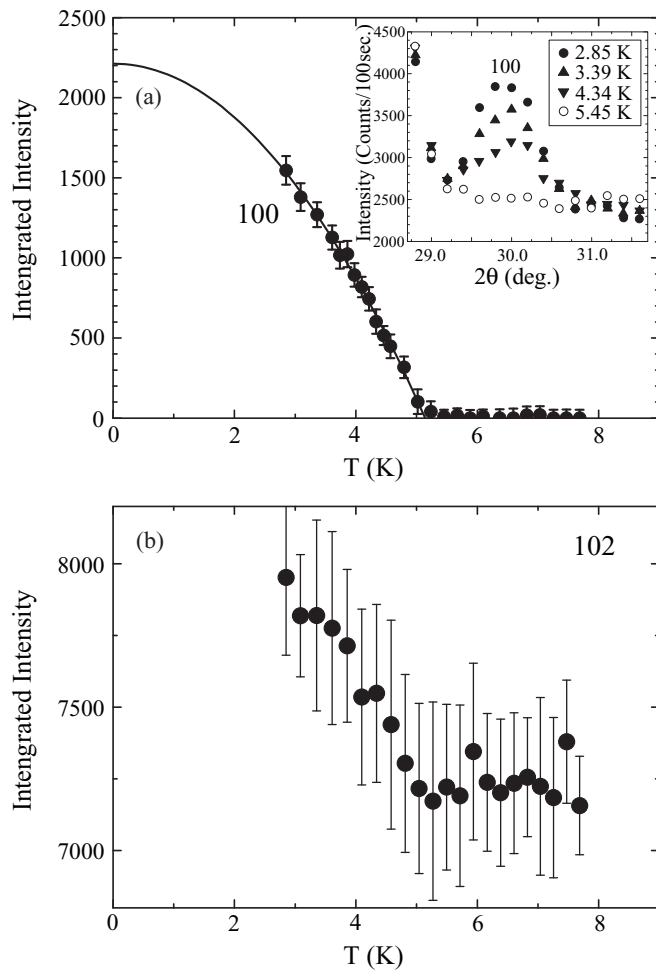| Nuclear Bragg at 11.2 K			Magnetic Bragg at 2.9 K		
hkl	I_{obs}	I_{cal}	*hkl*	I_{obs}	I_{cal}
001	8354(428)	10316	100	1579(128)	1594
002	8354(152)	8607			
101	759(93)	652			
102	7148(301)	7734	102	827(141)	715
003/110	3643(200)	3843			
111	7490(304)	5111	111	905(149)	1008
112	51380(951)	52171			
103	10002(325)	7569			
004	3626(108)	3520			
113/200	38757(1001)	40004			
201	2842(231)	2418	201	363(123)	200

FIG. 4. Temperature dependences of the integrated intensities of (a) 100 and (b) 102 reflections, respectively. The solid line shows the fitting the data below 5 K to the function that the intensity is proportional to $1 - (T/T_N)^2$ and the extrapolation of the fitting function to zero kelvin. In the inset : temperature dependence of the peak profile of 100 reflection.

of ∼200 in the calculation, the observed intensities cannot be estimated due to the experimental error, as mentioned above.

The inset of Fig. 4(a) is the temperature (T) dependence of the peak profile of 100 reflection. As shown in the inset, 100 reflection appears below 5.45 K and the peak gradually develops with decreasing T. Figures 4(a) and 4(b) show the T dependences of the integrated intensities of 100 and 102 reflections, respectively. The intensity of 102 reflection has a large error bar in this scale because this reflection includes the nuclear scattering. The intensities of both reflections increase with decreasing T below about 5 K, consistent with the temperature at which the jump of the specific heat is observed.[6] As shown in the main panel of Fig. 4(a), the temperature development of the magnetic Bragg intensity is monotonous down to 2.9 K and an anomaly is not observed at the superconducting transition temperature, 4.2 K. It is quite different from the behaviors observed in heavy fermion superconductors in which the magnetic ordering and the superconductivity coexist. For example, Cd-doped CeCoIn$_5$, CeCo(In$_{1-x}$Cd$_x$)$_5$ with $x = 0.1$ and 0.075, exhibit the

antiferromagnetic orderings of the Ce moment at Néel temperatures, $T_N \sim 3.0$ K and 2.5 K, respectively. Superconductivities appear below ∼1.2 and 1.7 K, and the antiferromagnetic ordering and the superconductivity coexist below these temperatures.[14] In these compounds, the magnetic Bragg peaks appear below T_N and their intensities increase with decreasing T. However, the developments of the magnetic Bragg intensities are suppressed and they become almost flat to the temperature below T_c.[15,16] The present T dependence of the magnetic Bragg intensity suggests that the Ce $4f$ electron is almost independent of the superconductivity and this compound is not a heavy fermion superconductor.

The solid line in Fig. 4(a) shows the fitting of data below 5.0 K to the function that the intensity is proportional to, $1 - (T/T_N)^2$, and the extrapolation of the fitting function to 0 K. The amplitude of the momtent at 0 K obtained by the fitting is 1.71 μ_B. In the experimental accuracy, any structural change is not observed and the tetragonal symmery remains down to 2.9 K. In the tetragonal symmetry, energy levels of the Ce $4f^1$ state split into three doublet states, $\Gamma_7^{(1)}$, $\Gamma_7^{(2)}$, and Γ_6, by the crytalline electric field, where the two former doubles consist of linear combination of $J_z = \pm 3/2$ and $J_z = \pm 5/2$ states, and the latter consists of $J_z = \pm 1/2$ state. In the case of CeAgSb$_2$ which also has a ZrCuSiAs-type structure, the ground state is the Γ_6 state, revealed by the measurement of the crystalline electric-field excitation. The amplitude of the antiferromagnetic ordered moment is in good agreement with $g_J \mu_B J_z \sim 0.43 \mu_B$.[17] On the other hand, the ordered moment in this compound is much larger than the moment of CeAgSb$_2$, indicating that the ground state of this compound is not the Γ_6 state. Such differences of the amplitude of the ordered moment and/or the ground state are caused by the differences of the structural parameters and constituent elements. Actually, other compounds with a ZrCuSiAs-type structure, CeCuBi$_2$ and CeAgBi$_2$, exhibit antiferromagnetic ordering with easy axes parallel to the c direction. Their saturated ordered moments which are estimated by magnetization curves are 1.76 and 2.1 μ_B, respectively. These behaviors are similar to the present compound while in CeCuBi$_2$ and CeAgBi$_2$, the superconductivity is not observed and their magnetization curves show metamagnetic behavior which is not observed in the present compound.

CeNi$_{0.8}$Bi$_2$ has the same crystal structure as the so-called 1111 system which has a maximum T_c of about 55 K among iron-based high-T_c superconductors. Theoretical studies on an iron-based high-T_c superconductor point out that magnetic fluctuation arising from a nesting between Fermi surfaces at Γ and M points in an unfolded Brillioun zone is an origin of the superconductivity.[18–21] Experimentally, strong correlations between the high-T_c superconductivity and the spin fluctuation are observed in an iron-based high-T_c superconductor. The inelastic neutron scattering measurements on LaFeAsO$_{1-x}$F$_x$ with $x = 0.057$, 0.082, and 0.157, show that the spin fluctuation observed in the samples with $x = 0.057$ and 0.082, whose T_c are about 30 K, almost disappears in the sample with $x = 0.157$ in which the high-T_c superconductivity is almost suppressed.[22] On the other hand, the superconductivity may appear without magnetic fluctuation in CeNi$_{0.8}$Bi$_2$, because Ni is nonmagnetic and the

Ce moment is almost decoupled with the superconducting carrier. The absence of the magnetic fluctuation may indicate that the T_c of $CeNi_{0.8}Bi_2$ is much lower than the values of iron-based superconductors although they have same crystal structures.

IV. SUMMARY

We have performed neutron powder diffraction measurements on a new superconductor, $CeNi_{0.8}Bi_2$, with $T_c \sim 4.2$ K. The structural parameters at room temperature are determined by the Rietveld method. The clear magnetic Bragg peaks are observed at $q = (0\ 0\ 0)$ below about 5 K. In the magnetic ordering phase, the two Ce moments in the unit cell are antiparallel along the c axis and the Ni atom does not contribute to the magnetic Bragg reflections. Below T_c,

the superconductivity and antiferromagnetic ordering coexist. The magnetic Bragg intensity monotonously increases with decreasing T below about 5 K and does not exbihit an apparent anomaly at $T_c \sim 4.2$ K, suggesting that the $4f$ electron of the Ce atom is almost independent of the superconductivity. The saturated ordered moment is about 1.7 μ_B.

[1] Y. Kamihara, T. Watanabe, M. Hirano, and H. Hosono, J. Am. Chem. Soc. **130**, 3296 (2008).

[2] M. Rotter, M. Tegel, and D. Johrendt, Phys. Rev. Lett. **101**, 107006 (2008).

[3] F.-C. Hsu, J.-Y. Luo, K.-W. Yeh, T.-K. Chen, T.-W. Huang, P. M. Wu, Y.-C. Lee, Y.-L. Huang, Y.-Y. Chu, D.-C. Yan, and M.-K. Wu, Proc. Natl. Acad. Sci. USA **105**, 14262 (2008).

[4] X. C. Wang, Q. Q. Liu, Y. X. Lv, W. B. Gao, L. X. Yang, R. C. Yu, F. Y. Li, and C. Q. Jin, Solid State Commun. **148**, 538 (2008).

[5] L. Fang, H. Yang, P. Cheng, X. Zhu, G. Mu, and H.-H. Wen, Phys. Rev. B **78**, 104528 (2008).

[6] H. Mizoguchi, S. Matsuishi, M. Hirano, M. Tachibana, E. Takayama-Muromachi, H. Kawaji, and H. Hosono, Phys. Rev. Lett. **106**, 057002 (2011).

[7] H. Flandorfer, O. Sologub, C. Godart, K. Hiebl, A. Leithe-Jasper, P. Rogl, and H. Noël, Solid State Commun. **97**, 561 (1996).

[8] A. Thamizhavel, A. Galatanu, E. Yamamoto, T. Okubo, M. Yamada, K. Tabata, T. C. Kobayashi, N. Nakamura, K. Sugiyama, K. Kindo, T. Takeuchi, R. Settai, and Y. Ōnuki, J. Phys. Soc. Jpn. **72**, 2632 (2003).

[9] M. H. Jung, A. H. Lacerda, and T. Takabatake, Phys. Rev. B **65**, 132405 (2002).

[10] H. Kito, H. Eisaki, and A. Iyo, J. Phys. Soc. Jpn. **77**, 063707 (2008).

[11] F. Izumi and T. Ikeda, Mater. Sci. Forum **321-324**, 198 (2000).

[12] Magnetic susceptibility of $CeNi_{0.8}Bi_2$ can be fitted by the Curie–Weiss law in the temperature range of $30 \leqslant T \leqslant 300$ K. From the Curie constant, the effective moment is 2.80 μ_B, which corresponds

to the effective moment of single-crystal $CeNiBi_2$, 2.88 μ_B and 2.60 μ_B for $H \parallel a$ and $H \parallel c$, reported in Ref. 8. These values are larger than 2.54 μ_B of a free Ce^{3+} ion. However, if the Ni atom has a local moment and also contributes to the Curie–Weiss-type susceptibility, the Curie constant and/or the effective moment have to be much larger than the observed values.

[13] P. J. Brown, *International Tables for Crystallography*, edited by A. J. C. Wilson (Kluwer Academic, Dordrecht, The Netherlands, 1992), Vol. C, Chap. 4.

[14] L. D. Pham, Tuson Park, S. Maquilon, J. D. Thompson, and Z. Fisk, Phys. Rev. Lett. **97**, 056404 (2006).

[15] M. Nicklas, O. Stockert, Tuson Park, K. Habicht, K. Kiefer, L. D. Pham, J. D. Thompson, Z. Fisk, and F. Steglich, Phys. Rev. B **76**, 052401 (2007).

[16] Sunil Nair, O. Stockert, U. Witte, M. Nicklas, R. Schedler, K. Kiefer, J. D. Thompson, A. D. Bianchi, Z. Fisk, S. Wirth, and F. Steglich, Proc. Natl. Acad. Sci. USA **107**, 9537 (2010).

[17] S. Araki, N. Metoki, A. Galatanu, E. Yamamoto, A. Thamizhavel, and Y. Ōnuki, Phys. Rev. B **68**, 024408 (2003).

[18] I. I. Mazin, D. J. Singh, M. D. Johannes, and M. H. Du, Phys. Rev. Lett. **101**, 057003 (2008).

[19] V. Cvetkovic and Z. Tesanovic, Europhys. Lett. **85**, 37002 (2009).

[20] K. Kuroki, S. Onari, R. Arita, H. Usui, Y. Tanaka, and H. Kontani, and H. Aoki, Phys. Rev. Lett. **101**, 087004 (2008).

[21] F. Ma and Z.-Y. Lu, Phys. Rev. B **78**, 033111 (2008).

[22] S. Wakimoto, K. Kodama, M. Ishikado, M. Matsuda, R. Kajimoto, M. Arai, K. Kakurai, F. Esaka, A. Iyo, H. Kito, H. Eisaki, and S. Shamoto, J. Phys. Soc. Jpn. **79**, 074715 (2010).